Design of Compact Wide Stopband Microstrip Low-pass Filter using T-shaped Resonator

Akram Sheikhi, Abbas Alipour, and Abdolali Abdipour, *Senior Member, IEEE*

***Abstract*— In this letter, a compact microstrip low-pass filter (LPF) using T-shaped resonator with wide stopband is presented. The proposed LPF has capability to remove the eighth harmonic and a low insertion loss of 0.12 dB. The bandstop structure using stepped impendence resonator and two open-circuit stubs are used to design a wide stopband with attenuation level better than −20 dB from 3.08 up to 22 GHz. The proposed filter with −3-dB cutoff frequency of 2.68 GHz has been designed, fabricated, and measured. The operating of the LPF is investigated based on equivalent circuit model. Simulation results are verified by measurement results and excellent agreement between them is observed.**

***Index Terms*— Low-pass filter (LPF), open stubs, T-shaped resonator, wide stopband.**

I. Introduction

In the modern wireless communication systems, microwave low-pass filter (LPF) is an essential component to suppression of spurious frequencies. The planar filters are popular structures because of their simple structures and low fabrication cost. The stepped impedance LPFs sustain from gradual cutoff frequency and narrow stopband [1]. To overcome this problem and design an LPF with wide stopband and high performance to suppress harmonics, different structures, such as stepped impendence resonators, defected ground structures, and electromagnetic bandgap, have been presented [2]–[8]. In [3] and [4], the stepped impendence hairpin resonators have been used to achieve LPFs with sharp roll-off and wide stopband. In [5] and [6], a microstrip LPF using coupled-line hairpin resonator has been proposed. However, this filter has gradual cutoff frequency. The LPF in [7] has disadvantages, such as circuit complexity and high insertion loss in the passband. In [8], the LPF using triangular and polygonal patches is presented. The LPF in [9], in spite of compact size, suffers from gradual cutoff frequency and low attenuation level in the stopband. In other studies, some configurations with good performance using T-shaped and open stubs in [10], and hexangular resonator in [11] were reported. In [12], an LPF with wide stopband and sharp roll-off rate has been presented, but the structure suffers from relatively high insertion loss and low return loss in the passband region. In this letter, a compact LPF using T-shaped resonator, bandstop structure and two open circuit stubs is presented, Fig. 1.

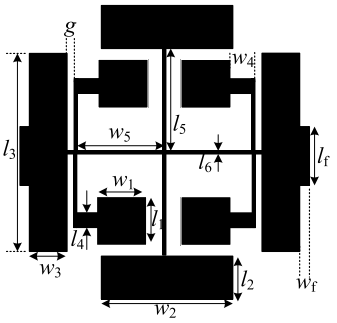

Fig. 1. Layout of the proposed LPF, $w_1 = 1.99$, $w_2 = 6$, $w_3 = 1.5$, $w_4 = 0.83$, $w_5 = 3.58$, $w_f = 0.4$, $l_1 = 2.06$, $l_2 = 1.99$, $l_3 = 7.96$, $l_4 = 0.6$, $l_5 = 3.93$, $l_6 = 0.1$, $l_f = 1.69$, and $g = 0.3$ (all in mm).

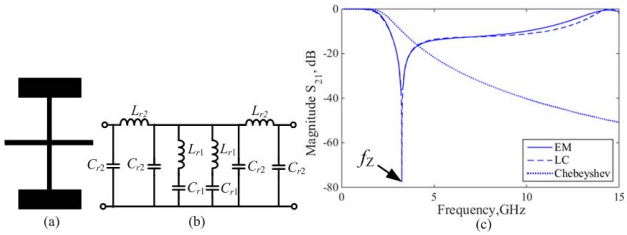

Fig. 2. (a) Layout of the resonator. (b) *LC* equivalent circuit ($L_{r1} = 2.35$ nH, $L_{r2} = 2.35$ nH, $C_{r1} = 1.02$ pF, and $C_{r2} = 0.103$ pF). (c) *LC* and EM simulation results.

II. Design Procedure

Fig. 2(a) shows the physical layout of the T-shaped resonator. The *LC* equivalent circuit of the T-shaped resonator is shown in Fig. 2(b). The equivalent elements L_{r1} and L_{r2} are the inductances of the high impedance transmission lines. C_{r1} and C_{r2} are the capacitances of the low impedance transmission lines and open-ended capacitances, respectively. The values of lumped elements can be extracted by the use of formula in [1] as $L = \sqrt{\varepsilon_{\text{eff}}} Z_c l/c$ and $C = \sqrt{\varepsilon_{\text{eff}}} l/c Z_c$, where Z_c is the characteristic impedance of the line, l is the length of line, c is the velocity of light in free space, and ε_{eff} is the effective dielectric constant. The calculated and optimized values for *LC* equivalent circuit of the proposed resonator are $L_{r1} = 2.95$ nH, $L_{r2} = 2.8$ nH, $C_{r1} = 1.54$ pF, $C_{r2} = 0.097$ pF and $L_{r1} = 2.35$ nH, $L_{r2} = 2.35$ nH, $C_{r1} = 1.02$ pF, $C_{r2} = 0.103$ pF, respectively.

The transmission zero (TZ) of the proposed structure is obtained from

$$Z = \frac{j\omega L_{r1} + \frac{1}{j\omega C_{r1}}}{2} \left\| \frac{1}{j2\omega C_{r2}} \right. = \frac{\frac{L_{r1}}{4C_{r2}} - \frac{1}{4\omega^2 C_{r1} C_{r2}}}{j\left(\frac{\omega L_{r1}}{2} - \frac{1}{2\omega C_{r1}} - \frac{1}{2\omega C_{r2}}\right)} \quad (1)$$

Manuscript received July 28, 2016; revised October 11, 2016; accepted October 28, 2016. Date of publication February 1, 2017; date of current version February 10, 2017.

A. Sheikhi and A. Alipour are with the Electrical Engineering Department, Lorestan University, Khorramabad, Iran (e-mail: akram.sheikhi2008@gmail.com; alipoor.ab@fe.lu.ac.ir).

A. Abdipour is with the Institute of Communications Technology and Applied Electromagnetics, and Micro/mm-wave and Wireless Communication Research Lab, Radio Communications Center of Excellence, Electrical Engineering Department, Amirkabir University of Technology, Tehran, Iran (e-mail: abdipour@aut.ac.ir).

Color versions of one or more of the figures in this paper are available online at http://ieeexplore.ieee.org.

Digital Object Identifier 10.1109/LMWC.2017.2652862

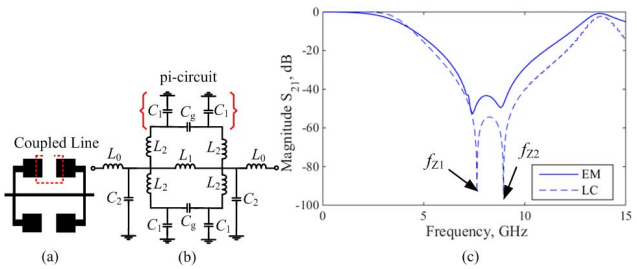

Fig. 3. (a) Layout. (b) *LC* equivalent circuit ($L_0 = 0.9$ nH, $L_1 = 4.14$ nH, $L_2 = 1.21$ nH, $C_1 = 0.3$ pF, $C_2 = 0.401$ pF, and $C_g = 1$ fF). (c) *LC* and EM simulation results of bandstop structure.

so

$$f_z = \frac{1}{2\pi\sqrt{L_{r1}C_{r1}}} = 3.25 \text{ GHz}. \tag{2}$$

It can be concluded from (2) that the location of the TZ at 3.25 GHz is a function of L_{r1} and C_{r1}, which changes with the length of l_5 and w_2, respectively. The capacitance of C_{r2} is low, so it has negligible impact on the location of TZ. Tuning the physical dimensions of the proposed resonator results in the desirable performance. The proposed resonator is designed based on a one-pole Chebyshev low-pass prototype with an insertion loss of 0.12 dB and $n = 3$. The element values of the low-pass Chebyshev prototype are obtained as $g_0 = 1$, $g_1 = g_3 = 0.84$, and $g_2 = 1.1$. The S_{21} parameters of the layout, Chebyshev prototype, and the *LC* equivalent circuit is shown in Fig. 2(c). As can be seen there is a good agreement between *LC* equivalent circuit, Chebyshev prototype, and frequency response of the layout. Unlike the conventional Chebyshev filter, the proposed resonator can generate a finite frequency TZ with a better selectivity by tuning L and C (physical dimension).

To improve the stop bandwidth, the structures in Fig. 3(a) have been added to the proposed resonator. The *LC* equivalent circuit, and a comparison between the *LC* and EM simulations are shown in Fig. 3(b) and (c). L_0, L_1, and L_2 and C_1, C_2, and C_g are the inductances and capacitances of the high-impedance lossless lines and capacitances of two-coupled lines and the low impedance lines. The values of these parameters can be calculated by the methods mentioned in [1]. The transfer function of the bandstop structure is calculated as (3)

where

$$Z_0 = \frac{1}{L_0 s}, \quad Z_1 = \frac{1}{L_0 s} + C_2 s + \frac{2}{L_2 s} + \frac{1}{L_1 s}, \quad Z_2 = \frac{1}{L_1 s}$$
$$Z_3 = 2C_g s, \quad Z_4 = 2C_g s + 2C_1 s + \frac{2}{L_2 s}, \quad Z_c = \frac{2}{L_2 s}$$

and r is characteristic impedance of the system. The TZs can be calculated by (3) as f_{z1} and f_{z2} at the top of the next page.

As can be seen, f_{z1} and f_{z2} are the function of pi-circuit (which consists of C_1 and C_g) and inductance L_1 and L_2. Also, the location of f_{z1} and f_{z2} is shown in Fig. 3(c). As shown in Fig. 3(c), the frequency responses of this bandstop structure exhibit a stopband ranging from 5.3 to 13 GHz with a rejection level better than -10 dB. By bandstop structure, a compact LPF with wide stopband can be implemented. Fig. 4(a)–(c) shows the layout, *LC* equivalent circuit, and frequency response of the primary filter. As expected by addition of bandstop structure, the attenuation level in the stopband region is increased by three TZs at 3.3, 7.1, and 9.8 GHz.

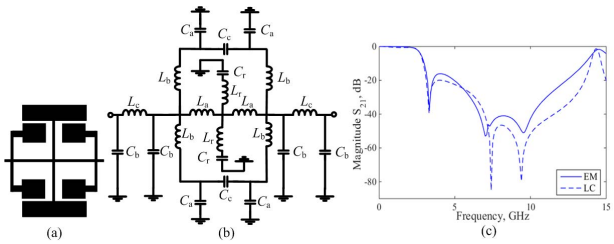

Fig. 4. (a) Layout. (b) *LC* equivalent circuit ($L_a = 2.35$ nH, $L_b = 1.21$ nH, $L_c = 0.9$ nH, $L_r = 2.35$ nH, $C_a = 0.3$ pF, $C_b = 0.5213$ pF, $C_c = 1$ fF, and $C_r = 1.01$ pF). (c) *LC* and EM simulation results of primary filter.

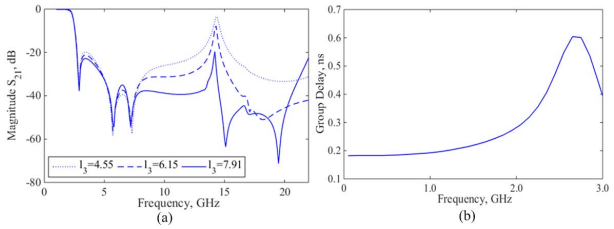

Fig. 5. (a) Magnitude of S_{21} parameter as a function of l_3. (b) Group delay.

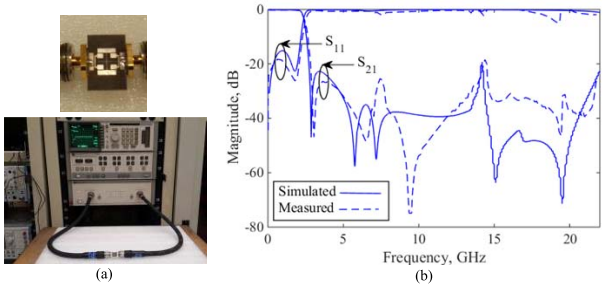

Fig. 6. (a) Photograph of the fabricated LPF and measurement setup. (b) Measured and simulated results of the fabricated LPF.

One of the main parameters of the resonator is cutoff frequency that can be changed with several parameters. In Table I, the cutoff frequency versus substrate thickness at different dielectric constant ε_r is shown. It is obvious that by variation of the substrate thickness and ε_r, we can tune the cutoff frequency of the resonator.

III. Fabrication of the Proposed LPF and Measurment Results

To achieve better performance in the aspect of attenuation level in the stopband region, two open-circuit stubs are added at the input and output of the proposed resonator. The frequency response and group delay of the LPF are

$$\frac{V_o}{V_i} = -\frac{r\left(Z_0 Z_3 Z_c^2 - Z_0 Z_2 Z_3^2 + Z_0 Z_2 Z_4^2\right)}{\left\langle\left(Z_1^2 - Z_2^2\right)\left(Z_3^2 - Z_4^2\right) - Z_c^4 + 2Z_c^2(Z_2 Z_3 + Z_1 Z_4)\right\rangle(r + L_0 s) + r\left\langle Z_0 Z_1\left(Z_4^2 - Z_3^2\right) - Z_0 Z_4 Z_c^2\right\rangle} \tag{3}$$

$$f_{Z1} = \frac{1}{2\pi} \times \sqrt{-\frac{\sqrt{C_g^2L_1^2 + C_g^2L_2^2 + 2C_gC_1L_1L_2 + 2C_g^2L_1L_2} - (C_1L_2 + C_gL_1 + C_gL_2)}{C_1^2L_2^2 + 2C_gC_1L_2^2}} = 7.73 \text{ GHz}$$

and

$$f_{Z2} = \frac{1}{2\pi} \times \sqrt{\frac{\sqrt{C_g^2L_1^2 + C_g^2L_2^2 + 2C_gC_1L_1L_2 + 2C_g^2L_1L_2} + (C_1L_2 + C_gL_1 + C_gL_2)}{C_1^2L_2^2 + 2C_gC_1L_2^2}} = 9 \text{ GHz}.$$

TABLE I

CUTOFF FREQUENCY VERSUS SUBSTRATE THICKNESS AT DIFFERENT DIELECTRIC CONSTANT VALUES

ε_r\thickness(mil)	10	15	20	25	30	35
2.2	2.21	2.44	2.68	2.7	2.79	2.86
2.65	2.03	2.24	2.4	2.51	2.59	2.67
3.38	1.82	2.02	2.19	2.27	2.34	2.42

TABLE II

COMPARISON OF THIS LETTER WITH OTHER LPFS

Ref	IL (dB)	RL (dB)	Stop Bandwidth (-20 dB)	Size (mm×mm)
[2]	1.5	11	2.8 GHz-10 GHz	70.68×13
[3]	0.4	20	1.38 GHz-5.5 GHz	22.4×24.05
[4]	0.5	16.3	0.8 GHz-4.6 GHz	34.62×70.95
[5]	0.45	14	3.2 GHz-11.8 GHz	0.7×12.9 3.4×12.9
[7]	0.6	12	2.8 GHz-15 GHz	25×10
[8]	0.3	15	2 GHz-9 GHz	11×19
[9]	0.36	16	2.2 GHz-12.4 GHz	17×15.6
[11]	0.8	9	1.37 GHz-16 GHz	15×35
This Work	0.12	18.5	3.08 GHz-22 GHz	12.4×11.9

shown in Fig. 5(a)–(b). As can be seen from Fig. 5(a), by increasing the length l_3, suppression of harmonic at 14.2 GHz increases. As can be seen from Fig. 5(b), the group delay of the LPF in the passband region is lower than 0.62 ns. The measurement setup, and the photograph of fabricated LPF and measurement results are shown in Fig. 6(a) and (b). Two microstrip lines with the dimensions of W_f and L_f are used for 50-Ω matching. A wide stopband with -20 dB attenuation level from 3.08 to 22 GHz is observed. The proposed filter is fabricated on the substrate with a relative dielectric constant of 2.2, a thickness of 20 mil, and a loss tangent of 0.0009 and simulated and optimized using ADS 2014 simulator tool and measured by the HP 8510B network analyzer.

The proposed filter has a -3-dB cutoff frequency equal to 2.68 GHz, insertion loss 0.12 dB in the passband, return loss 18 dB, and suppression level better than -20 dB from 3.08 up to 22 GHz; thus, the proposed LPF has a property of eighth-harmonic suppression and very good performance. Table II summarizes the performance of some published LPFs. As shown in Table II, the proposed filter exhibits a wide stopband, low insertion loss, and good return loss among the quoted filters.

IV. CONCLUSION

A novel compact microstrip LPF with T-shaped resonator and open-circuit stubs with new configuration was designed, fabricated, and measured. Results show that the proposed LPF achieves good features, such as wide stopband, and sharp transition band in the stopband region, low insertion loss, and good return loss in the passband region as well as compact size. Considering these characteristics, the proposed LPF can be used in the communication systems.

REFERENCES

[1] J. S. Hong and M. J. Lancaster, *Microstrip Filters for RF/Microwave Applications*. New York, NY, USA: Wiley, 2001.

[2] S.-W. Ting, K.-W. Tam, and R. P. Martins, "Miniaturized microstrip lowpass filter with wide stopband using double equilateral U-shaped defected ground structure," *IEEE Microw. Wireless Compon. Lett.*, vol. 16, no. 5, pp. 240–243, May 2006.

[3] L. Li, Z.-F. Li, and J.-F. Mao, "Compact lowpass filters with sharp and expanded stopband using stepped impedance hairpin units," *IEEE Microw. Wireless Compon. Lett.*, vol. 20, no. 6, pp. 310–312, Jul. 2010.

[4] V. K. Velidi and S. Sanyal, "Sharp roll-off lowpass filter with wide stopband using stub-loaded coupled-line hairpin unit," *IEEE Microw. Wireless Compon. Lett.*, vol. 21, no. 6, pp. 301–303, Jun. 2011.

[5] S. Luo, L. Zhu, and S. Sun, "Stopband-expanded low-pass filters using microstrip coupled-line hairpin units," *IEEE Microw. Wireless Compon. Lett.*, vol. 18, no. 8, pp. 506–508, Aug. 2008.

[6] F. Wei, L. Chen, and X.-W. Shi, "Compact lowpass filter based on coupled-line hairpin unit," *Electron. Lett.*, vol. 48, no. 7, pp. 379–381, Mar. 2012.

[7] J.-L. Li, S.-W. Qu, and Q. Xue, "Compact microstrip lowpass filter with sharp roll-off and wide stop-band," *Electron. Lett.*, vol. 45, no. 2, pp. 110–111, Jan. 2009.

[8] L. Ge, J. P. Wang, and Y.-X. Guo, "Compact microstrip lowpass filter with ultra-wide stopband," *Electron. Lett.*, vol. 46, no. 10, pp. 689–691, May 2010.

[9] H. Cui, J. Wang, and G. Zhang, "Design of microstrip lowpass filter with compact size and ultra-wide stopband," *Electron. Lett.*, vol. 48, no. 14, pp. 856–857, Jul. 2012.

[10] M. Hayati, M. Gholami, H. S. Vaziri, and T. Zaree, "Design of microstrip lowpass filter with wide stopband and sharp roll-off using hexangular shaped resonator," *Electron. Lett.*, vol. 51, no. 1, pp. 69–71, 2015.

[11] G. Karimi, A. Lalbakhsh, and H. Siahkamari, "Design of sharp roll-off lowpass filter with ultra wide stopband," *IEEE Microw. Wireless Compon. Lett.*, vol. 23, no. 6, pp. 303–304, Jun. 2013.

[12] M. Hayati and A. Abdipour, "Compact microstrip lowpass filter with sharp roll-off and ultra-wide stop-band," *Electron. Lett.*, vol. 49, no. 18, pp. 1159–1160, Aug. 2013.